Distributions of Welding Residual Stresses in Various Welded Joints of Thick Plates†

Yukio UEDA* and Keiji NAKACHO**

Abstract

It was ten and several years ago that the authors developed a theory and a method for theoretical analysis of welding transient and residual stresses produced in a multi-pass welded joint of a very thick plate. Several years later, they also proposed and established a general measuring theory for experimental measurement of three-dimensional residual stresses. Henceforth, using these methods, they have obtained transient and residual stresses produced in many kinds of welded joints. In this paper, these calculated and measured results being summarized, residual stresses of thick plates due to multi-pass welding are synthetically studied and discussed on the characteristics of distributions, the correlation with cold cracking, the mechanism of production, etc.

KEY WORDS: (Welding Residual Stress) (Multi-pass Welding) (Theoretical Analysis) (Experimental Measurement) (Influencing Factor) (Cold Crack) (Welded Joint) (Thick Plate)

1. Introduction

For study of safety of welded structures, it is very important to know transient and residual stresses produced by multi-pass welding in thick plates. However, it had been very difficult to obtain them by theoretical analysis or experimental measurement, owing to complexity of mechanical behaviors of weld metal and HAZ, three-dimensional state of stresses, etc.

More than ten years ago, the authors started a research on multi-pass welding residual stresses by performing theoretical analysis. In this research, based on the theories of thermal elastic-plastic analysis (finite element method)[1),2)], they developed an efficient and accurate method[3)–6)] for analysis of multi-pass welding transient and residual stresses. Applying this method, multi-pass welding transient and residual stresses have been obtained, and their production mechanisms, their relations with cold cracks, etc. have been clarified[3)–14)]. About ten years ago, they proposed a new measuring theory of three-dimensional residual stresses using inherent strain as a parameter[5),15)] and developed actual measuring methods such as L_z method[16),17)] and L_y method[17),18)]. It became practically possible to measure multi-pass welding residual stresses. Henceforth, welding residual stresses of several welded joints have been measured by newly developed approaches based on this theory[16),17),19)].

In this paper, using the results of these theoretical analysis and experimental measurement, characteristics of distribution of multi-pass welding residual stresses, influencing factors on them and their relations with cold cracks are discussed synthetically.

2. Characteristics of Residual Stress Distributions, Influential Factors and Their Relations with Cold Cracks in Multi-pass Welded Joints

2.1 Calculated welding residual stresses

The authors have analyzed transient and residual stresses produced in various types of multi-pass welded joints of thick plates by theoretical method, and the production mechanisms of such stresses, the relations with cold cracks, etc. have been investigated[3)–14)]. A simple joint model under simple welding condition (SM 50 butt welded joint of 50 mm thickness plane plate) is chosen as an appropriate example (first example) to describe the characteristics of distributions of residual stresses. In the theoretical analyses treated in this section, temperature or temperature-history dependence of mechanical properties of materials are considered.

2.1.1 Multi-pass butt welded joint of thick plane plate (SM 50, plate thickness: 50 mm)

As shown in **Fig. 1**, 20-layer (20-pass) narrow gap butt welding was applied to SM 50 steel plate of 50 mm thickness[6)]. It was considered that the distribution pattern depends on the restraint condition of a joint, and two extreme restraint conditions were assumed; a condition under which longitudinal deformation and angular distortion occur freely (restraint condition A) and one under which both deformations are restricted (restraint condition B). Under respective conditions, residual stresses were

† Received on April 28, 1986
* Professor
** Research Instructor

Transactions of JWRI is published by Welding Research Institute of Osaka University, Ibaraki, Osaka 567, Japan

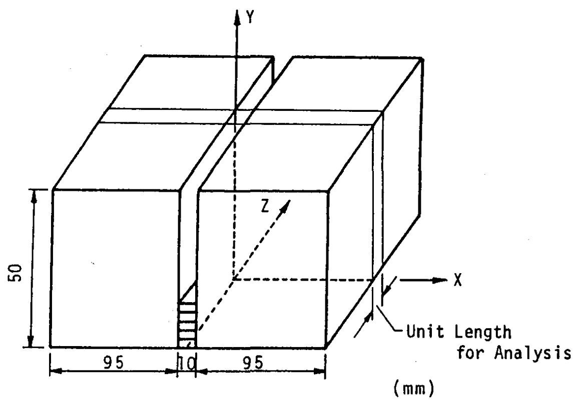

Fig. 1 Specimen for Analysis.

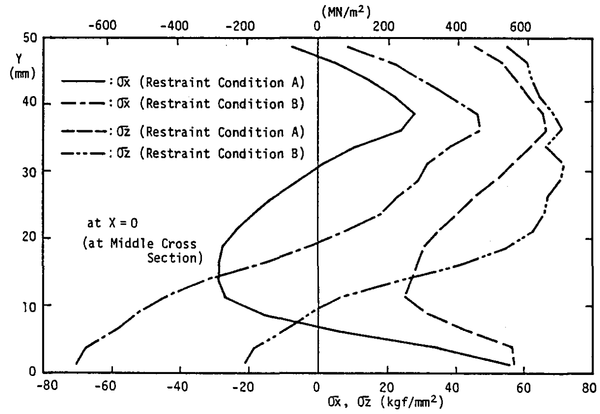

(a) At the Middle Cross Section

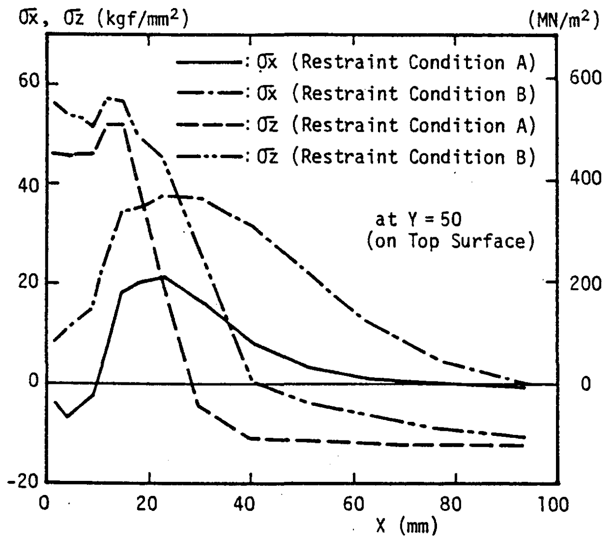

(b) On the Top Surface

Fig. 2 Calculated Welding Residual Stresses.

obtained by theoretical analysis.

Distributions of residual stresses in the middle cross section of the weld zone and on the top surface of the specimen are shown in **Fig. 2**. σ_x indicates stresses in the plate width direction and σ_z those along the weld line. In case of restraint condition A in which longitudinal deformation and angular distortion occur freely, residual stresses near the bottom surface of the weld zone become largely tensile both along the weld line and in the plate width direction. In case of restraint condition B in which the above-mentioned deformations are restrained, these stresses are converted to compressive ones. Accordingly, root crack may occur under very small degree of restraint.

On the other hand, the effect of restraint condition was relatively small on the top surface side, i.e., in the vicinity of the finishing bead. The reason is that as the plate thickness increases, the above-mentioned deformations are more restrained internally when the welding near the finishing bead is applied, because the weld metal already laid recovers rigidity. The distribution of residual stresses near the finishing bead may be characterized by that the maximum tensile stresses appear not on the finishing bead but several layers below (see Refs. 4 and 7 for this reason). This is remarkable in plate width direction. Large tensile residual stresses in this vicinity may cause underbead crack, longitudinal crack and transverse crack.

2.1.2 Cylinder-head welded joint of a pressure vessel of very thick plates (2¼Cr-1Mo steel, plate thickness: 100, 150 mm)

Welding residual stresses produced in a cylinder-head joint (U-groove) of a pressure vessel (**Fig. 3 (a)**) made of very thick 2¼Cr-1Mo steel plate were estimated[3)–5),7)]. For analysis and experiment, double U-groove joint models (**Fig. 3 (b)**) of 200 and 300 mm plate thickness which are twice as thick as the original were prepared, since it was considered that longitudinal deformation and angular distortion hardly occur due to the high degree of internal structural restraint for the actual joint. Each pass of welding was applied to these models alternately on each side of the grooves. In the experiment, submerged arc welding was applied. The numbers of passes were 87 for Model M-200 of 200 mm plate thickness and 167 for Model M-300 of 300 mm plate thickness.

Shown in **Fig. 4** are the transverse welding transient and residual stresses σ_x on the top surface and in the middle cross section of Model M-300 obtained by both theoretical analysis and experiment. If attention is paid to residual stresses, it is seen that their distributions are subjected to the effect of restraint. Like the case of a butt joint of a plane plate under restraint condition B of the previous example, compressive stresses remain in the middle of the plate thickness direction (corresponds to the inner surface of an actual joint), the initially welded portion, and tensile stresses are produced near the top surface, of which maximum value appears just under the finishing bead. If embrittlement due to diffusive hydrogen accompanies, underbead crack may occur and expand to the surface.

Transient stresses produced when the groove is welded

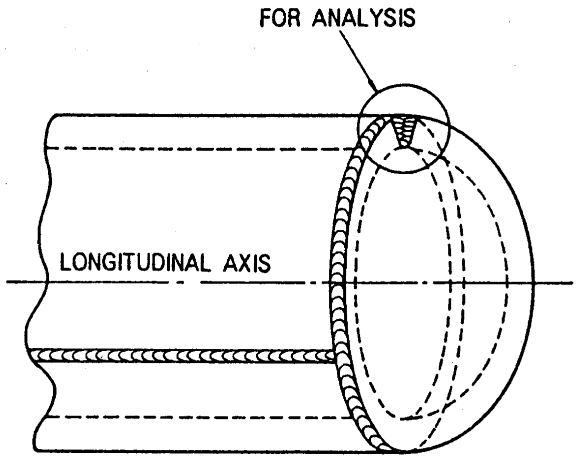

(a) Cylinder-head Welded Joint

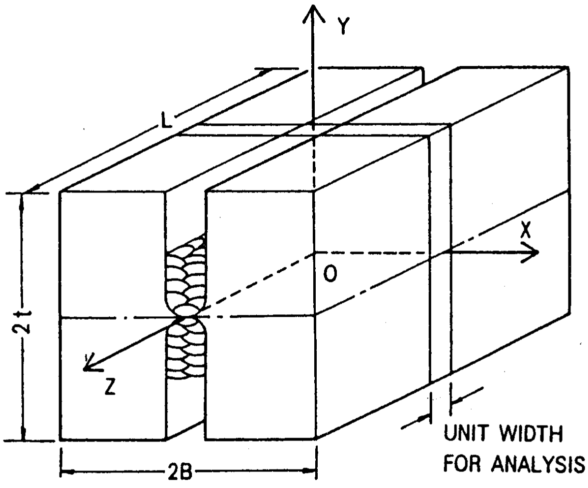

(b) Idealized Research Model

Fig. 3 Cylinder-head Welded Joint of a Pressure Vessel and Its Research Model.

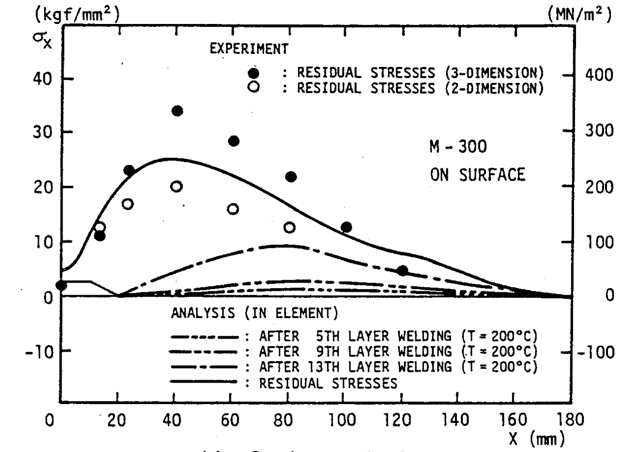

(a) On the Top Surface

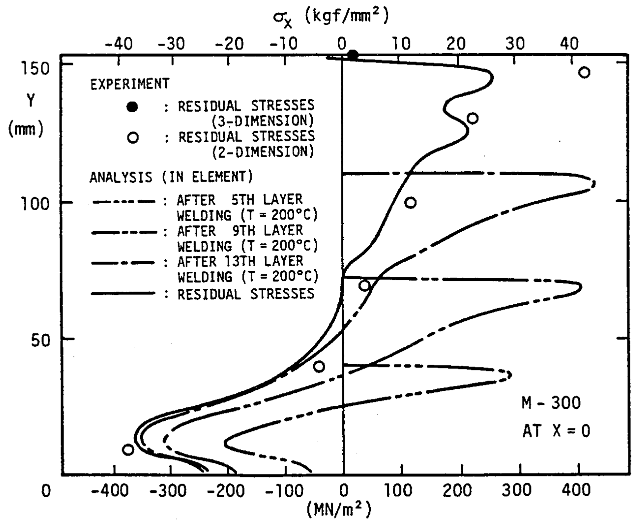

(b) At the Middle Cross Section

Fig. 4 Transverse Welding Transient and Residual Stresses.

halfway and cooled to the interpass temperature (200°C) are also shown in Fig. 4. The pattern of these distributions shows fundamentally the same characteristics as of the aforementioned residual stresses.

2.1.3 Multi-pass corner welded joint of thick plane plate (SM 50, plate thickness: 40 mm)

In order to investigate and prevent lamellar tearing and root crack of a multi-pass corner joint from a dynamical view point, welding residual stresses produced in such a joint have been analyzed under various conditions[8)–11)]. CJC (Corner Joint weld Cracking) test model shown in **Fig. 5** was used for the analysis of a corner joint. Changing the external restraint, theoretical analyses were performed for the cases when bending restraint intensity is large ($K_B = 10^6$ kgf·mm/mm·rad) and when it is the least ($K_B = 0$).

Shown in **Fig. 6** are the distributions of welding residual stresses σ_x (perpendicular to the weld line) in the section of the weld zone and on the top surface of the vertical plate. These distributions change in a similar

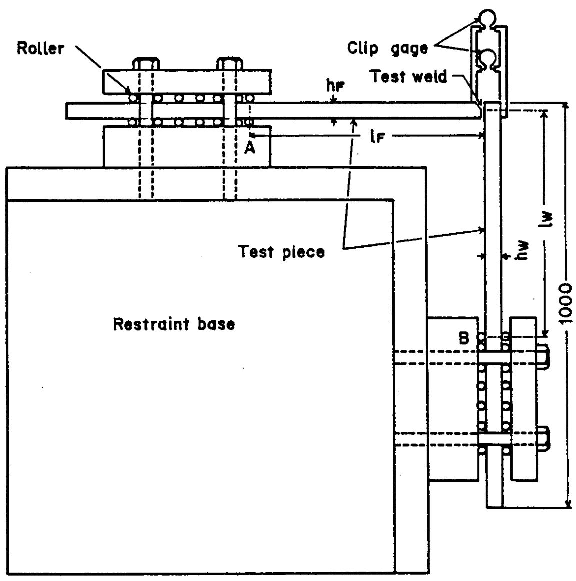

Fig. 5 Corner Joint Weld Cracking Test (CJC-test) Apparatus.

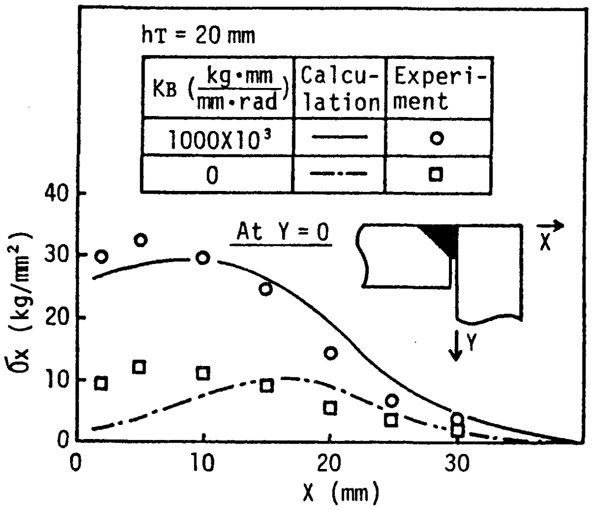

(a) On the Top Surface (At Y = 0)

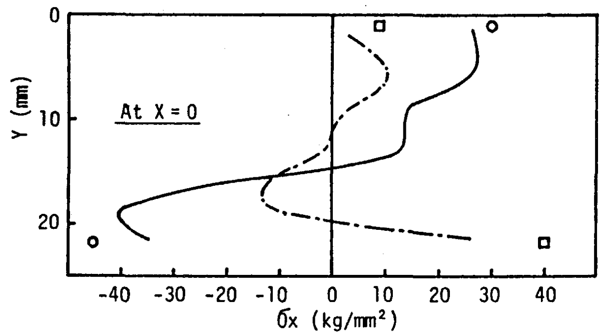

(b) At the Cross Section (At X = 0)

Fig. 6 Transverse Welding Residual Stresses.

manner to those in the butt joint of the first example according to the change of restraint to angular distortion (corresponds to bending restraint here). When bending restraint is large, tensile residual stresses on the top surface of the vertical plate become larger and may cause lamellar tearing. When bending restraint is small, large tensile stresses are produced at the root of the groove and may cause root crack.

With the purpose to prevent initiation of lamellar tearing by decreasing tensile stresses on the top surface of the vertical plate even when bending restraint is large, residual stresses were analyzed on four types of groove (**Fig. 7**). Residual stress distributions near the top surface of the vertical plate are shown in **Fig. 8**. Tensile residual stresses of types P and C are smaller than those of type M.

2.1.4 Multi-pass butt welded joint of thin and thick pipes (SUS 304, plate thickness: 5.5, 8.6 and 30.9 mm)

Residual stresses produced in SUS 304 steel pipes by circumferential multi-pass butt welding (V-groove) were theoretically analyzed[12)–14)]. Sizes of the used pipes are 2B pipe (5.5 mm thickness), 4B pipe (8.6 mm) and 24B pipe (30.9 mm), and the sequence of welding is shown in **Fig. 9**. TIG welding method was applied to the welding of initial passes and SMAW to the sequent passes. From the

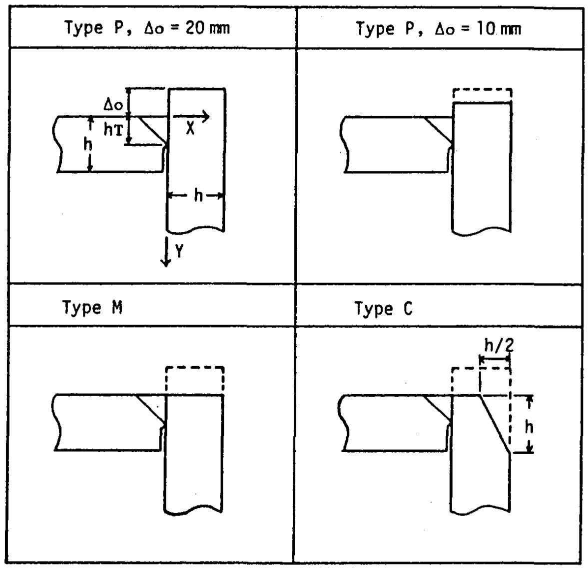

h = 40 mm, hT = 20 mm, Angle of vee : 45°
KB = 1000X10³ kg·mm/mm·rad (l = 56 mm)

Fig. 7 Shapes of Grooves.

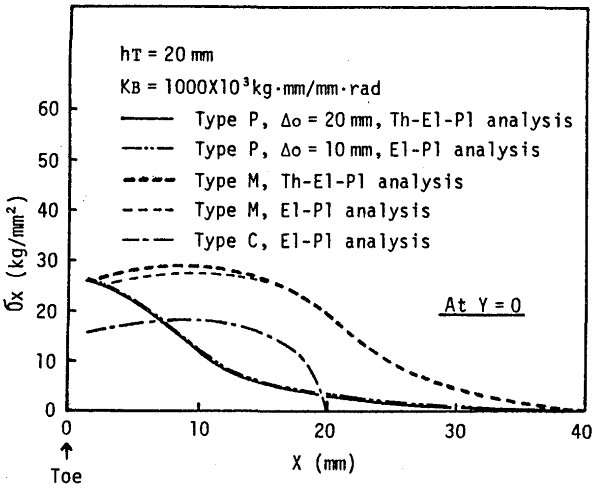

Fig. 8 Calculated Transverse Welding Residual Stresses on the Top Surface.

third layer, the heat-sink welding by which the inner surface of a weld zone is cooled by strong water-spraying during welding was applied in addition to the conventional welding by which a joint is naturally cooled. This heat-sink welding aims to produce compressive residual stresses on the inner surface of the weld zone and prevent stress corrosion cracking. 4B pipe was also used to investigate how the influence differs when heat input is increased and the number of passes is decreased. Analyzed residual stress distributions are shown in **Figs. 10** (heat input is increased to Q-14, Q-23, Q-45) and **11**.

Since butt welded joints of pipes are axisymmetric, longitudinal deformation due to welding is internally restrained, while angular distortion occurs to some degree. In case of 24B pipe (30.9 mm thickness), stress distributions are similar to one produced under this restraint condition. That is, the distributions are between those

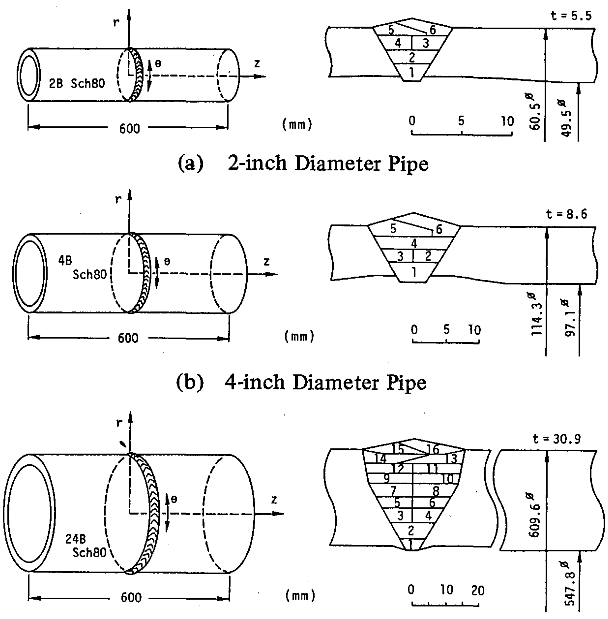

(a) 2-inch Diameter Pipe

(b) 4-inch Diameter Pipe

(c) 24-inch Diameter Pipe

Fig. 9 Dimensions and Build-up Sequences of Pipes Used in Analysis.

produced under the two extreme restraint conditions of the butt joint of the first example.

If heat-sink welding is used, the inner surface or the initially welded side is compulsorily cooled, so that a great temperature difference occurs in the plate thickness direction like the case of thick plates. Therefore, even in case of thin plates such as 2B pipe (5.5 mm) and 4B pipe (8.6 mm), residual stresses distribute similarly to those in the restraint condition B of the butt joint of thick plates of the first example, and compressive stresses remain on the inner surface of the weld zone. These compressive stresses prevent stress corrosion cracking.

2.2 Measured welding residual stresses

The authors presented a general measuring principle of three-dimensional residual stresses in which inherent strain is used as a parameter and formulated it using the finite element method[5),15)]. Applying this measuring theory, they conducted experiments on several multi-pass butt welded joints of thick plates and measured their three-dimensional welding residual stresses. Followings are the examples[16),19)].

2.2.1 Multi-pass butt welded joint of thick plane plate (SS 41, plate thickness: 50 mm)

In experiment, residual stresses of a multi-pass butt welded joint (**Fig. 12**) of a mild steel (SS 41) plate were measured[16)]. The size of the used specimen is as follows: weld length, L = 200 mm, plate width B = 200 mm and plate thickness, t = 50 mm. 14-pass submerged arc welding

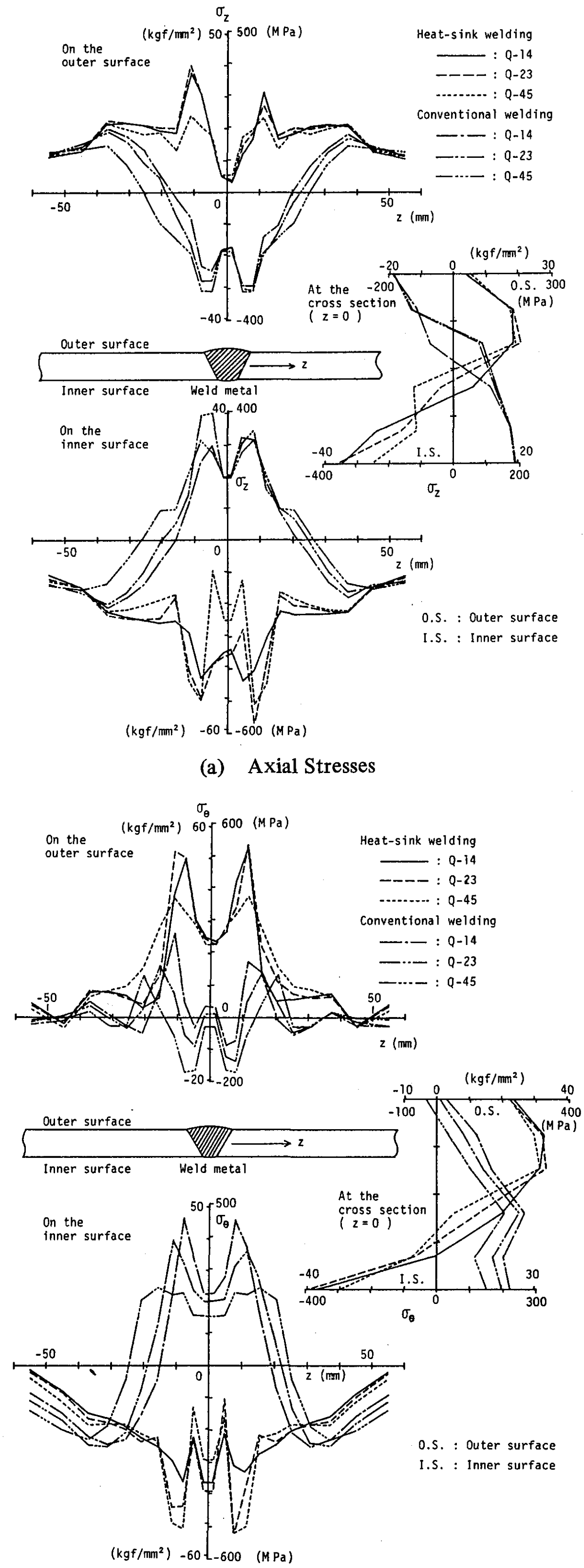

(a) Axial Stresses

(b) Circumferential Stresses

Fig. 10 Calculated Welding Residual Stresses of 4-inch Pipes on the Inner and Outer Surfaces and at the Middle Cross Section.

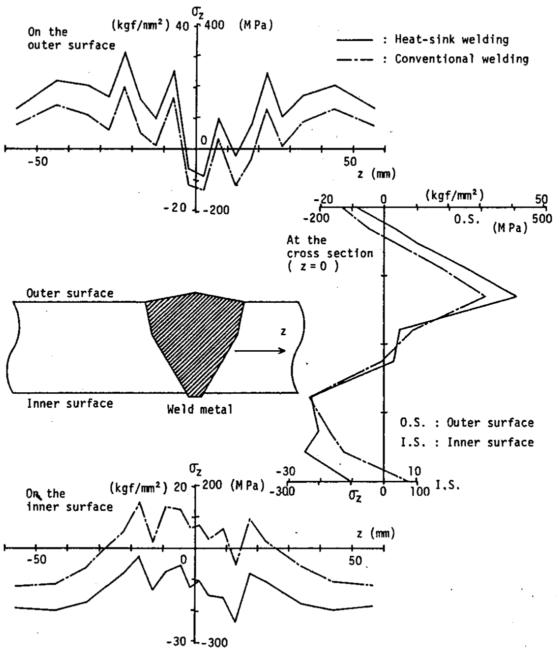

(a) Axial Stresses

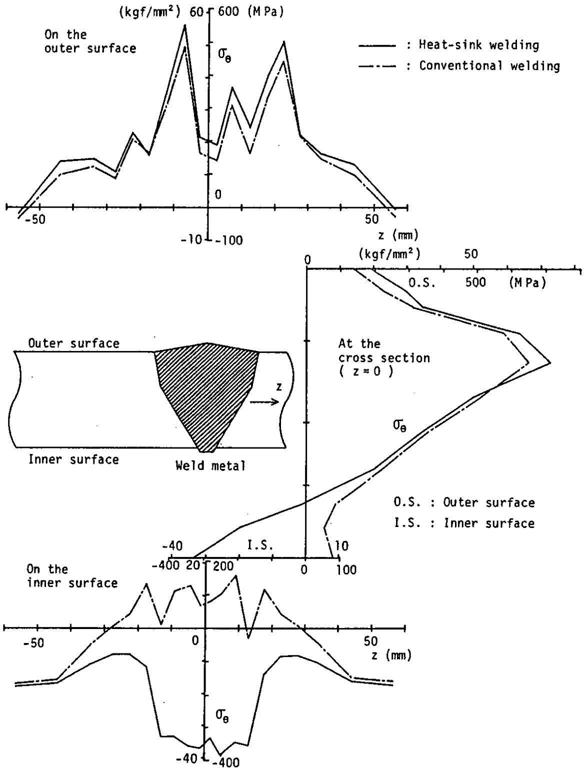

(b) Circumferential Stresses

Fig. 11 Calculated Welding Residual Stresses of 24-inch Pipes on the Inner and Outer Surfaces and at the Middle Cross Section.

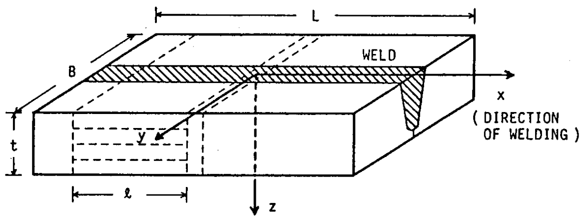

(a) Experimental Model of Multi-pass Welded Joint (R-specimen)

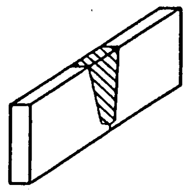

(b) Sliced Cross Section in the Weld Line (T-specimen)

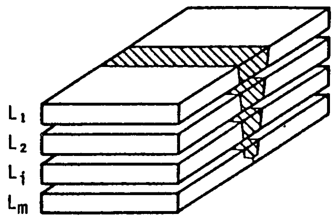

(c) Sliced Plates, Parallel to XY-plane (L_i specimen)

Fig. 12 Experimental Model and Procedure of Slicing T and L_i Specimens (L_z Method).

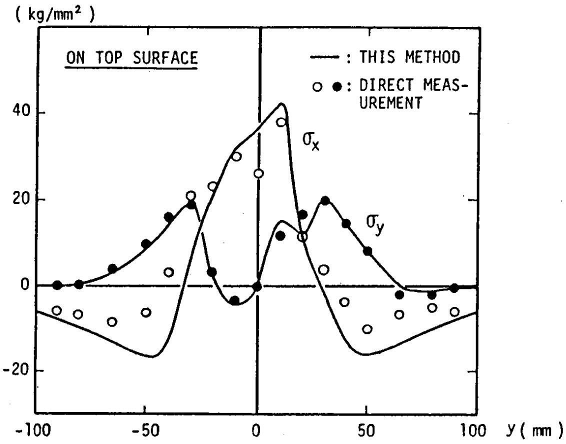

(a) On the Top Surface

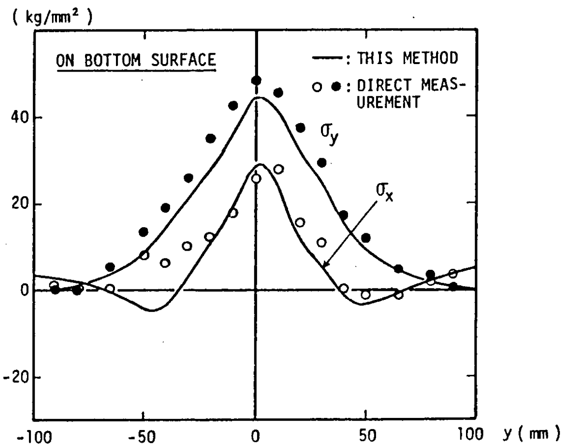

(b) On the Bottom Surface

Fig. 13 Measured Welding Residual Stresses on the Surfaces in the Middle of the Weld Line.

was applied to the U-groove of the specimen. No restraint was added to the welding deformation such as longitudinal deformation or angular distortion.

Residual stress distributions of σ_x (longitudinal direction) and σ_y (plate width direction) measured on the top and bottom surfaces and in the cross sections in the middle of the weld line are shown in **Figs. 13** and **14.** Their distribution patterns are quite the same as those under the restraint condition A of the joint of the first

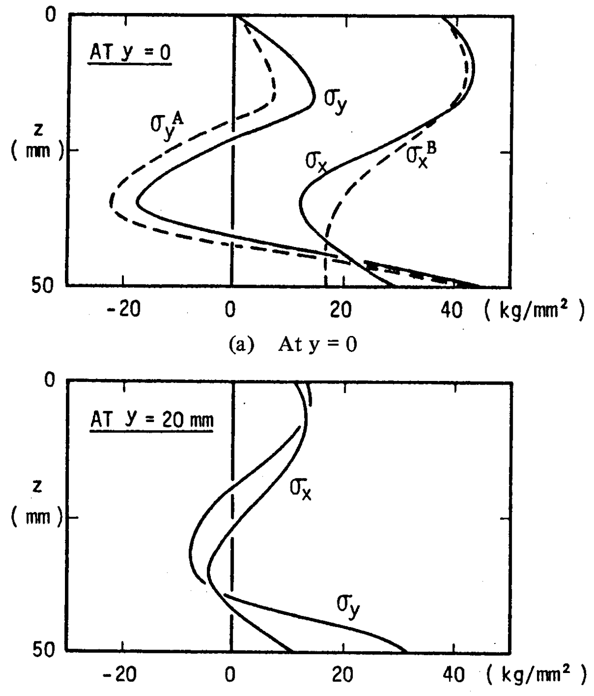

(a) At y = 0

(b) At y = 20 mm

Fig. 14 Measured Welding Residual Stresses at the Cross Section in the Middle of the Weld Line.

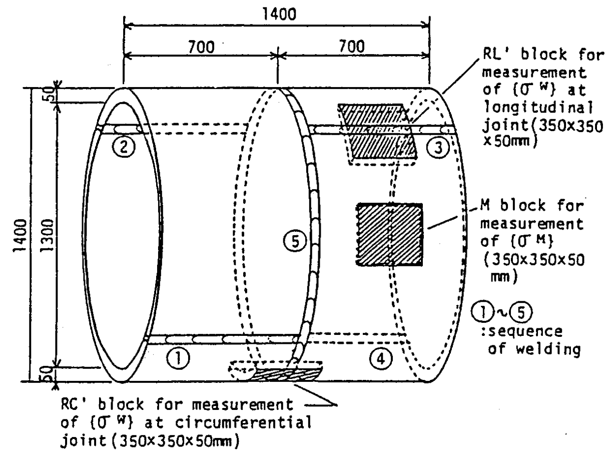

Fig. 15 Model of Penstock.

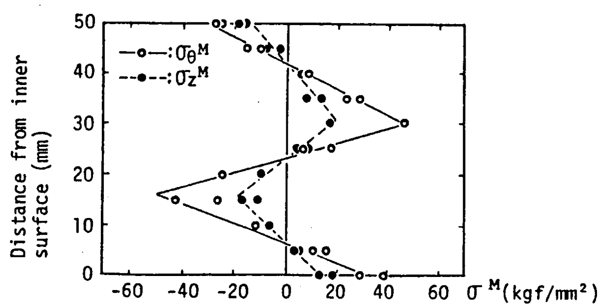

Fig. 16 Measured Residual Stresses due to Cold Bending in Shell Plate.

example, in which no external restraint is added. That is to say, large tensile stresses are produced not only immediately under the finishing bead but also at the bottom surface owing to the great influence of longitudinal deformation and angular distortion. This is one of the typical characteristics of the residual stress distributions. Accordingly, root crack may occur in this case.

2.2.2 Multi-pass butt longitudinal and circumferential welded joints in a penstock (HT 80, plate thickness: 50 mm)

Using a large size penstock model of 80 kgf/mm^2 class high tensile strength steel plate, three-dimensional residual stresses produced in a tubular shell plate by (1) cold bending, (2) longitudinal welding of a joint and (3) circumferential welding of a joint were measured respectively[19]. The penstock model and the location of each specimen taken out are shown in **Fig. 15**. The plate thickness of the model is 50 mm. Submerged arc welding was applied first to the inner side and then to the outer side of the X-grooves.

Distributions of three-dimensional residual stresses produced in the shell plate by cold bending are shown in **Fig. 16**. Residual stresses in the axial direction of the model, $\sigma_z{}^M$, and those in the circumferential direction, $\sigma_\theta{}^M$, are almost point-symmetric with respect to the center of the plate thickness. $\sigma_z{}^M$ is approximately 30 ~ 50% of $\sigma_\theta{}^M$ in magnitude. It is considered that these are the typical characteristics of residual stress distributions by this type of cold bending.

Welding residual stress distributions in the longitudinal joint are shown in **Figs. 17** and **18**. Distributions in Fig. 17 are complicated since welding residual stresses distribute on and near the weld metal, and combined residual stresses by cold bending and the subsequent weldings on the base plate near the weld line. The above residual stresses distributed in the plate thickness direction are shown in Fig. 18. Figure 18 (a) shows welding residual stresses in the weld zone and (b) residual stresses by cold bending and the subsequent weldings in the base plate. From these distributions, especially Fig. 18 (a), in reference to the first example, welding deformation behavior of this joint is predicted as follows: Angular distortion occurs easily in longitudinal joints as is evident from the distribution of $\sigma_\eta{}^W$ (circumferential stress) in Fig. 18 (a). While longitudinal deformation, which is considered to occur hardly, is known to considerably occur from the distribution of $\sigma_\xi{}^W$ (axial stress, along the weld line here) in the same figure. This may be explained by the fact that the length of the model at the longitudinal welding is shorter in comparison to the radius.

Distributions of welding residual stresses in a circumferential joint are shown in **Figs. 19** and **20**. It is seen from the residual stress distributions in the plate thickness direction of the weld zone shown in Fig. 20 (a) that distributions of circumferential (along the weld line) stresses $\sigma_\xi{}^W$ and axial stresses $\sigma_\eta{}^W$ are similar to those in the cir-

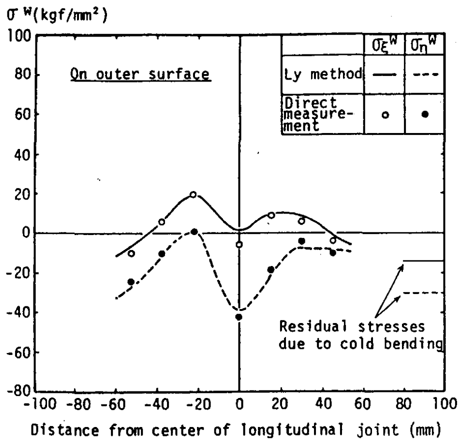

(a) On the Outer Surface

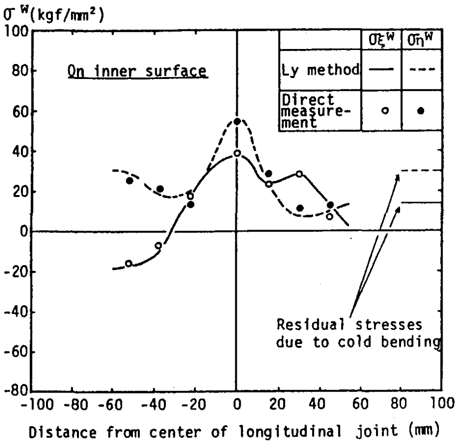

(b) On the Inner Surface

Fig. 17 Measured Welding Residual Stresses on the Surfaces (Longitudinal Joint).

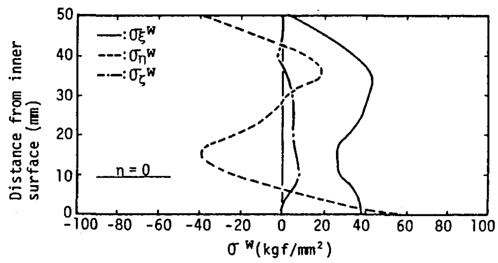

(a) $\eta = 0$

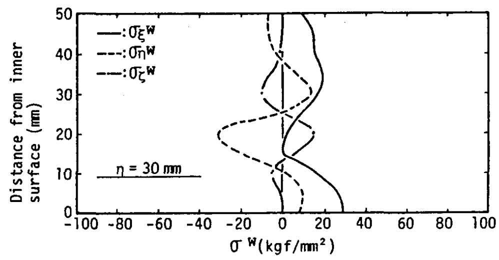

(b) $\eta = 30$ mm

Fig. 18 Measured Welding Residual Stresses at the Cross Sections (Longitudinal Joint).

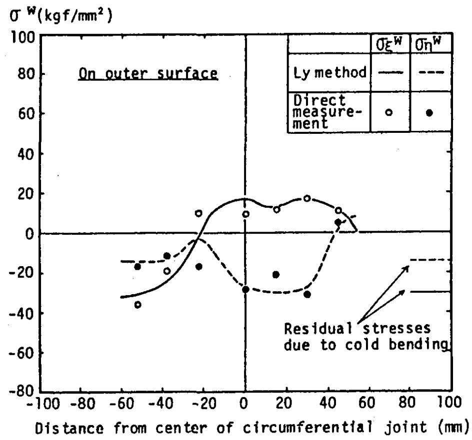

(a) On the Outer Surface

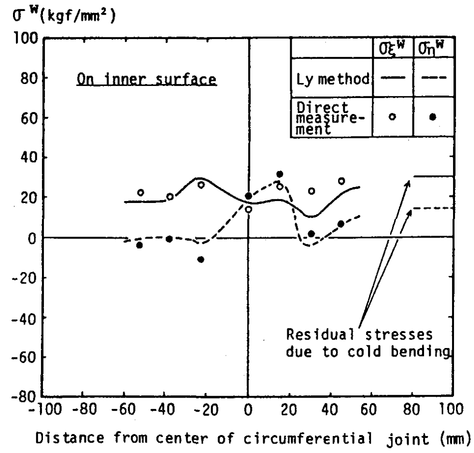

(b) On the Inner Surface

Fig. 19 Measured Welding Residual Stresses on the Surfaces (Circumferential Joint).

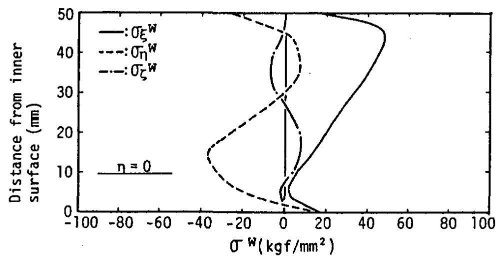

(a) $\eta = 0$

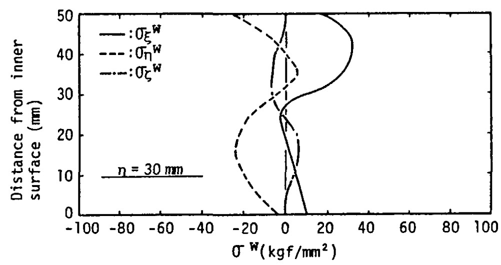

(b) $\eta = 30$ mm

Fig. 20 Measured Welding Residual Stresses at the Cross Sections (Circumferential Joint).

cumferential butt joint of 24B pipe already described in 2.1.4. Especially, σ_ξ^W shows a close resemblance to those in 24B pipe. Naturally, their production mechanisms are the same. It is considered that angular distortion occurs to some extent and longitudinal deformation little.

2.2.3 Butt welded joint of very thick plate by electroslag welding (SM 50, plate thickness: 100 mm)

Residual stresses of a butt welded joint of SM 50 steel of 100 mm plate thickness by electroslag welding (**Fig. 21**) were measured[17]. Electroslag welding takes quite a different welding process from multi-pass welding which has been treated in this study. Residual stresses by electroslag welding deserve attention as those produced by applying large heat input (2094 KJ/cm) for the single pass.

Welding residual stresses at the middle cross section of the weld line produced by this welding method are shown in **Figs. 22** and **23**. Figure 22 (a) shows the distributions of residual stresses in the plate width direction (y-direction) on the surface, Fig. 22 (b) those along the center of the plate thickness, and Fig. 23 the distributions of residual stresses in the plate thickness direction. The residual stress along the weld line, σ_x, shown in Fig. 22 (b) is comparatively similar to that produced in a one-pass butt welded joint made of a thin steel plate in which phase transformation occurs at a low temperature[20]. That is to say, of the distribution in the plate width direction, large tensile stresses are produced in the HAZ and small tensile stresses in the weld metal. The maximum tensile stresses are produced at the center of the plate thickness as seen from the distributions in the plate thickness direction at the HAZ (y = 50 mm) shown in Fig. 23 (b). The reason may be that the specimen is made of very thick plates so that the center of the plate thickness cools more slowly than any other portions.

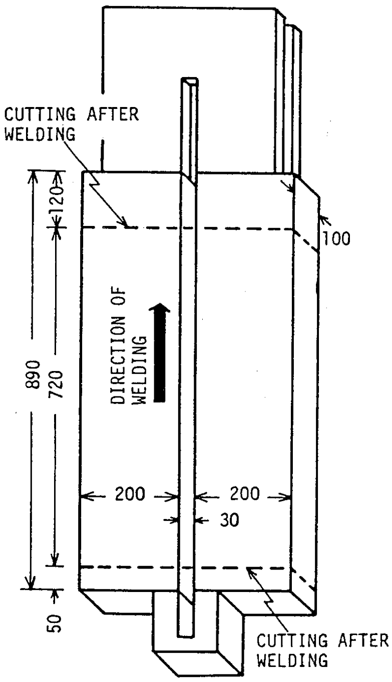

Fig. 21 Test Joint of Electroslag Welding.

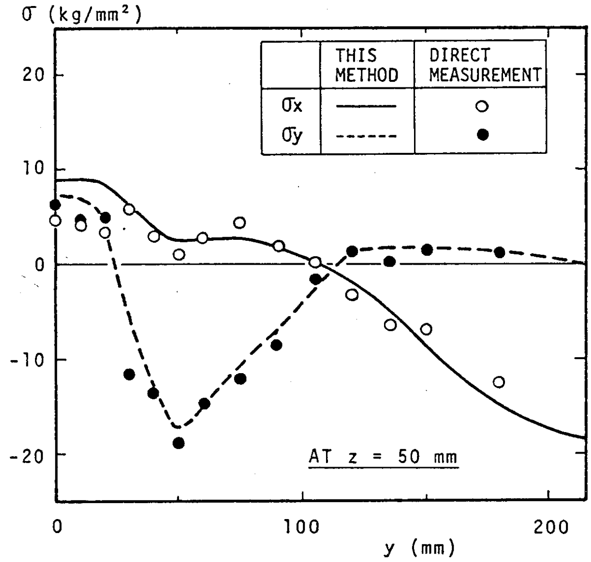

(a) On the Surface (At z = 50 mm)

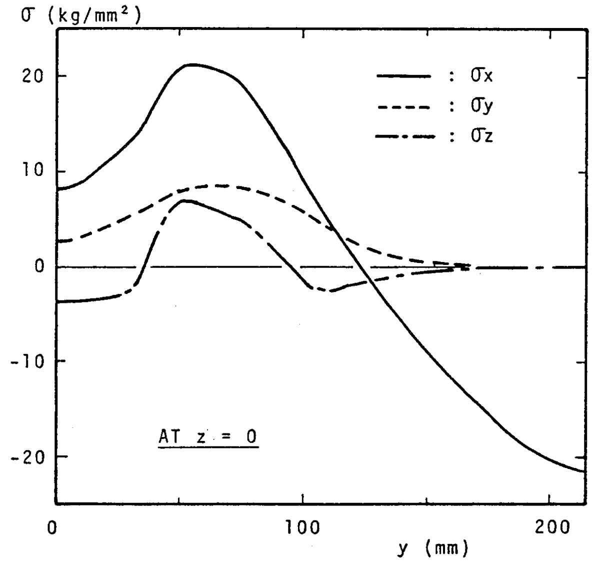

(b) Along the center of the Plate Thickness (At z = 0)

Fig. 22 Measured Welding Residual Stresses at the Middle Cross Section of the Weld Line.

2.3 Characteristics of residual stress distributions in multi-pass welded joints of thick plates and influential factors

Characteristics of residual stress distributions in several kinds of multi-pass welded joints of thick plates described in this research are summarized in the following.

Conceivable influential factors on the residual stress distributions are the followings:

(i) material properties (physical and mechanical properties), (ii) welding condition (especially heat input), (iii) groove shape, (iv) build-up sequence, (v) restraint

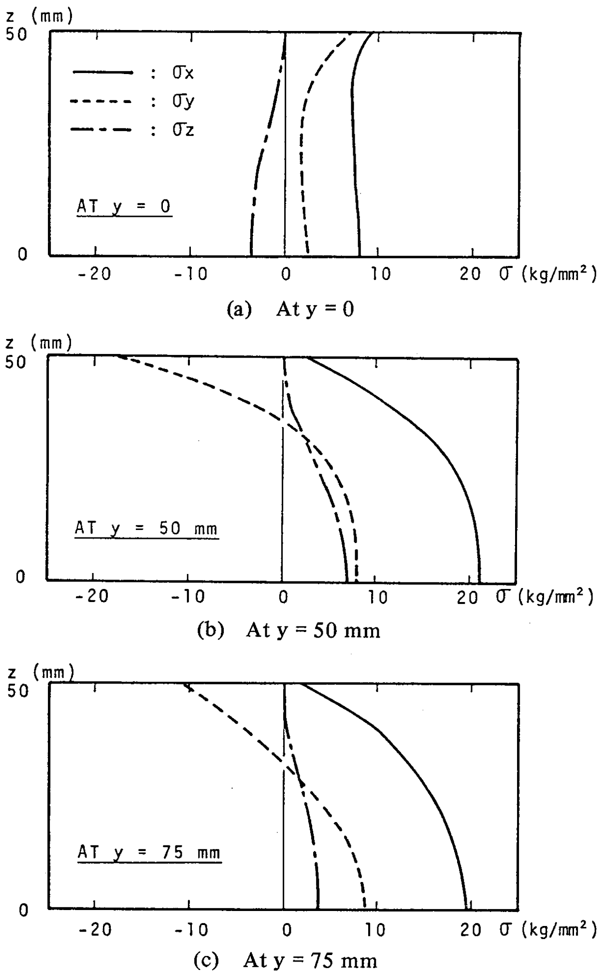

Fig. 23 Measured Welding Residual Stresses at the Middle Cross Section of the Weld Line (Distributions in the Plate Thickness Direction).

condition of a joint, etc.

Materials used for the joint models were; (a) SM 50, (b) 2¼Cr-1Mo, (c) SUS 304, (d) SS 41 and (e) HT 80.

Their mechanical properties, the aforementioned (i), such as yield stress, instantaneous linear expansion coefficient, etc., and their changes during phase transformation are greatly different from one another. So are (ii) the welding condition, (iii) the groove shape and (iv) the build-up sequence of the respective joints. These factors influence the welding residual stresses quantitatively. For example, in the joints made of HT 80 described in 2.2.2, the maximum residual stresses do not reach the yield stress. This is due to the phase transformation expansion at low temperature (400 ~ 500°C), which reduces the maximum tensile residual stresses greatly. However, as having already mentioned hereinbefore, the patterns of residual stress distributions are influenced a little by (i) material properties, (ii) the welding condition, (iii) the groove shape and (iv) the build-up sequence, while they are greatly influenced by and dependent on (v) the restraint condition of a joint. Therefore, such characteristics of residual stress distributions were arranged with respect to the restraint condition of a joint as shown in **Table 1**.

Correlations of the restraint condition of a joint with residual stress distributions and welding cracks may be simply stated as follows: "Irrespective of severity of the restraint condition of a joint, longitudinal and transverse (in the directions of the weld line and the plate width) large tensile stresses are produced in the surrounding portion of the finishing bead. These tensile stresses may cause underbead crack, longitudinal crack or transverse crack. If the restraints against longitudinal deformation and angular distortion are weak, large tensile residual stresses are produced near the initially welded bottom surface and may cause root crack."

As a result, the characteristics of residual stress distributions can be read qualitatively in this Table, provided that the restraint condition of a joint is estimated.

3. Concluding Remarks

In this research, the authors summarized residual stress distributions in multi-pass welded joints of thick plates obtained by theoretical analysis and experimental measurement on seven kinds of weld joints. They clarified correlations between the influential factors and cold cracks.

The most important conclusion is that the characteristics of residual stress distributions are greatly influenced by the restraint condition of a joint. Obtained correlations are shown in Table 1. From now on, it is possible to qualitatively know the characteristics of residual stress distributions from this Table if the restraint condition of a joint is estimated. The production mechanisms of the welding residual stresses of the joints, which were discussed only a little in this paper, are detailed in the papers written on respective joints.

References

1) Y. Ueda and T. Yamakawa: Analysis of Thermal Elastic-plastic Stress and Strain during Welding by Finite Element Method, Trans. of JWS (The Japan Welding Society), Vol. 2, No. 2, 1971, pp. 90–100, and IIW Doc. X-616-71, 1971, and Journal of JWS, Vol. 42, No. 6, 1973, pp. 567–577 (in Japanese).

2) Y. Ueda and K. Nakacho: Theory of Thermal Elastic-plastic Analysis with a More General Work Hardening Rule, Trans. of JWRI (Welding Research Institute of Osaka Univ., Japan), Vol. 9, No. 1, 1980, pp. 107–114, and IIW Doc. X-989-81, 1981.

3) Y. Ueda et al.: Analysis of Thermal Elastic-plastic Stresses and Strains due to Welding – Multi-layer Welds –, Proc. of 7th National symp. of Matrix Methods of Structural Analysis and Design (The Society of Steel Construction of Japan), 1973, pp. 419–426 (in Japanese).

4) Y. Ueda et al.: Transient and Residual Stresses in Multi-pass

Table 1 Classification of Welding Residual Stress Distributions According to the Restraint Condition.

Longitudinal Deformation		Angular Distortion: Restricted	Angular Distortion: ~	Angular Distortion: Free
	Restricted	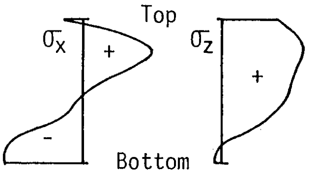 •Butt Joint of Plane Plate (SM50), Restraint Cond. B (1st Example) •Cylinder-Head Butt Joint of Pressure Vessel •Corner Joint of Plane Plate, $K_B=10^6$ kgf·mm/mm·rad	•Butt Joint of 24B Pipe •Butt Joint in Penstock, Circumferential Joint	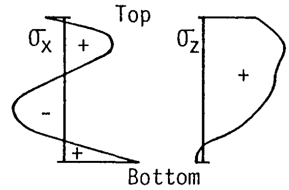
	) (			•Butt Joint in Penstock, Longitudinal Joint
	Free	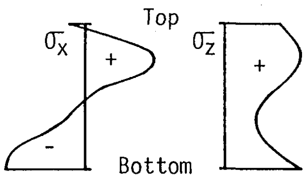		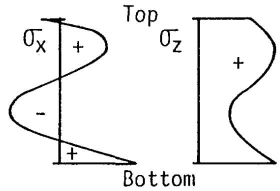 •Butt Joint of Plane Plate (SM50), Restraint Cond. A (1st Example) •Corner Joint of Plane Plate, $K_B=0$ •Butt Joint of Plane Plate (SS41)

σ_x : Transverse Welding Residual Stress, σ_z : Longitudinal Welding Residual Stress

Welds, IIW Doc. X-698-73, 1973, and Trans. of JWRI, Vol. 3, No. 1, 1974, and J. of JWS, Vol. 44, No. 6, 1975, pp. 464–474 (in Japanese).

5) Y. Ueda, K. Fukuda and K. Nakacho: Basic Procedures in Analysis and Measurement of Welding Residual Stresses by the Finite Element Method, Proc. of Int. Conf. on Residual Stresses in Welded Construction and Their Effects (The Welding Institute, England), 1977, pp. 27–37.

6) Y. Ueda and K. Nakacho: Simplifying Methods for Analysis of Transient and Residual Stresses and Deformation due to Multipass Welding, Trans. of JWRI, Vol. 11, No. 1, 1982, pp. 95–103, and Quarterly J. of JWS, Vol. 2, No. 1, 1984, pp. 75–82 (in Japanese).

7) Y. Ueda et al.: Multipass Welding Stresses in Very Thick Plates and Their Reduction from Stress Relief Annealing, IIW Doc. X-850-76, 1976, and Trans. of JWRI, Vol. 5, No. 2, 1976, pp. 179–189, and Proc. of Third Int. Conf. on Pressure Vessel Technology (ASME), Part II, 1977, pp. 925–933.

8) Y. Ueda et al.: Dynamical Characteristics of Weld Cracking in Multipass Welded Corner Joint, Trans. of JWS, Vol. 8, No. 2, 1977, pp. 138–142, and J. of JWS, Vol. 48, No. 1, 1979, pp. 34–39 (in Japanese).

9) Y. Ueda et al.: Prevention of Lamellar Tearing in Multipass Welded Corner Joint, Trans. of JWS, Vol. 9, No. 2, 1978, pp. 128–133, and J. of JWS, Vol. 48, No. 7, 1979, pp. 525–531 (in Japanese).

10) Y. Ueda et al.: Weld Cracking in Multipass Welded Corner Joint –Comparison of Submerged Arc Welding with Covered Arc Welding–, J. of JWS, Vol. 50, No. 4, 1981, pp. 421–427 (in Japanese), and IIW Doc. IX-1236-82 and X-1010-82, 1982.

11) Y. Ueda et al.: Cracking in Welded Corner Joints, Metal Constr., Vol. 16, No. 1, 1984, pp. 30–34.

12) Y. Ueda et al.: Residual Stresses at Circumferential Weld of Austenitic Strainless Steel Pipe by Heat-sink Welding, J. of JWS, Vol. 49, No. 1, 1980, pp. 61–66 (in Japanese).

13) Y. Ueda et al.: Residual Stresses and Their Mechanisms of Production at Circumferential Weld by Heat-sink Welding, J. of JWS, Vol. 52, No. 2, 1983, pp. 90–97 (in Japanese).

14) Y. Ueda, K. Nakacho and T. Simizu: Improvement of Residual Stresses of Circumferential Joint of Pipe by Heat-sink Welding for IGSCC, 1984 Pressure Vessel and Piping Conference (ASME), 84-PVP-10, 1984, and J. of Pressure Vessel Technology (ASME), Vol. 108, No. 1, 1986, pp. 14–23.

15) Y. Ueda et al.: A New Measuring Method of Residual Stresses with the Aid of Finite Element Method and Reliability of Estimated Values, J. of SNAJ (The Society of Naval Architects of Japan), Vol. 138, 1975. pp. 499–507 (in Japanese), and Trans. of JWRI, Vol. 4, No. 2, 1975, pp. 123–131, and IIW Doc. X-810-76, 1976.

16) Y. Ueda, K. Fukuda and M. Tanigawa: New Measuring Method of 3-dimensional Residual Stresses Based on Theory of Inherent Strain, J. of SNAJ, Vol. 145, 1979, pp. 203–211 (in Japanese), and Trans. of JWRI, Vol. 8, No. 2, 1979, pp. 249–256, and IIW Doc. X-987-81, 1981.

17) Y. Ueda, K. Fukuda and M. Fukuda: A Measuring Theory of Three Dimensional Residual Stresses in Long Welded Joints, J. of JWS, Vol. 49, No. 12, 1980, pp. 845–853 (in Japanese), Trans. of JWRI, Vol. 12, No. 1, 1983, pp. 113–122, and IIW Doc. X-1066-84, 1984.

18) Y. Ueda and K. Fukuda: Simplified Measuring Methods of Three Dimensional Welding Residual Stresses, Trans. of JWRI, Vol. 11, No. 2, 1982, pp. 95–104, and IIW Doc. X-1067-84, 1984.

19) Y. Ueda et al.: Three Dimensional Cold Bending and Welding Residual Stresses in Penstock of 80 kgf/mm^2 Class High Strength Steel Plate, J. of JWS, Vol. 51, No. 7, 1982, pp. 570–577 (in Japanese), and Trans. of JWRI, Vol. 12, No. 2, 1983, pp. 117–126, and IIW Doc. X-1068-84, 1984.

20) K. Satoh and T. Terasaki: Effect of Transformation Expansion on Welding Residual Stresses Distributions and Welding Deformations, J. of JWS, Vol. 45, No. 7, 1976, pp. 560–566 (in Japanese).